

Anthropogenic Geomorphological Changes in the Coastal area of Ain Al-Sokhna in Egypt, Using Remote Sensing and GIS

Dr. Islam Saber Amin Desouky

Assistant Professor, Department of Geography
Faculty of Arts, Benha University
islam.saber198@gmail.com

Dr. Heba Saber Amin Desouky

Assistant Professor, Department of Geography
Faculty of Arts, Benha University
hebasaber84@yahoo.com

doi: 10.21608/jfpsu.2024.248750.1312

Anthropogenic Geomorphological Changes in the Coastal area of Ain Al-Sokhna in Egypt, Using Remote Sensing and GIS

Abstract

Ain Sokhna in Egypt has undergone profound anthropogenic geomorphological shifts, driven by the establishment of the Sokhna port, tourist resorts, industrial facilities, and transportation routes. These alterations, closely linked to the region's strategic importance since the early 2000s, have essentially turned it into a hub for various industries. The construction of the Sokhna port caught the attention of various sectors, leading to the development of infrastructure and the transformation of the area into an attractive destination for tourism. Despite their human origin, these features are intricately connected to natural processes like erosion and sedimentation, causing noticeable changes in the morphology of the study area. While these human-induced activities have altered Ain Sokhna's coastal landscape, they have also yielded economic advantages, job opportunities, and infrastructural advancements. Striking a balance between development and environmental sustainability remains a formidable challenge for policymakers and local communities in the region, to address this challenge, it is imperative to conduct thorough studies, maintain ongoing monitoring efforts, and adopt sustainable coastal management practices. These measures are crucial to minimizing the adverse impacts of human activities and ensuring the long-term ecological health of Ain Sokhna.

Keywords: Ain Sokhna, Anthropogenic geomorphological changes, Sokhna port, Tourism development, Industrial facilities.

التغيرات الجيومورفولوجية البشرية بمنطقة العين السخنة الساحلية – مصر، باستخدام الاستشعار عن بعد ونظم المعلومات الجغرافية

مستخلص

شهدت منطقة العين السخنة تغيرات جيومورفولوجية بشرية ملحوظة خاصة مع إنشاء ميناء العين السخنة والمنتجعات السياحية والمنشآت الصناعية وتطوير شبكة الطرق ، حيث يمكن اعتبار هذه التغيرات مرتبطة ارتباطاً وثيقاً بالأهمية الاستراتيجية للمنطقة التي بدأت مع بداية العقد الأول من القرن الحادي والعشرين، وعلي الرغم من الأصل البشري لتلك الظواهر إلا أنها ترتبط ارتباطاً وثيقاً بالعمليات الطبيعية بما يسبب تغيرات ملحوظة في شكل منطقة الدراسة. وفي حين أن هذه الأنشطة قد غيرت من مورفولوجية منطقة العين السخنة، إلا أنها حققت أيضاً مزايا اقتصادية وفرص عمل وتطورات في البنية التحتية ، و يشكل التوازن بين التنمية والاستدامة البيئية تحدياً هائلاً يواجه صانعي القرار ، ولمواجهة هذا التحدي، لا بد من إجراء دراسات شاملة تتعلق بالمراقبة المستمرة، والإدارة الساحلية المستدامة، حيث تعتبر هذه الدراسات حاسمة لتقليل الآثار الضارة للأنشطة البشرية وضمان الاستدامة البيئية السليمة لمنطقة الدراسة على المدى الطويل .

الكلمات المفتاحية: العين السخنة، التغيرات الجيومورفولوجية البشرية، ميناء السخنة، التنمية السياحية، المنشآت الصناعية.

1- Introduction

Time moves in one direction, so morphological changes are the dominant characteristic of any form of the Earth's surface, especially dynamic forms. Geographically, these changes vary in terms of the time scales that they occurs on. Therefore, they are divided into short-term morphological changes that can be noticed within a few minutes or days through field measurements or direct visual observation, and intermediate-term morphological changes, which represent an interstitial stage of the study of morphological changes that can extend between several months to decades This is based on the comparative study of different-aged aero, satellite images, or maps. Finally, there are long-term morphological changes that occur over periods ranging from decades to millions of years, which can be monitored through geomorphological and archgeomorphological evidence.

The scope of anthropogenic geomorphology includes not only the study of man-made landforms, but also the study of man-caused geomorphological changes, and the prediction of the natural consequences of disturbed natural balances. When defining the scope and tasks of anthropogenic geomorphology, it cannot be neglected that most human structures are located in an environment in which natural processes are active and sometimes even pose a threat to human constructions; human society tries to defend itself against them. In this effort its tries to prevent or deter natural geomorphological processes and this is how you contribute to geomorphological development or change (Szabó, 2010).

The current study is concerned with intermediate-term morphological changes, where morphological changes attributed to anthropogenic activities are one of the main drivers for these changes, especially in areas that are affected by human interventions. The study is based on satellite images for the years 1984, 1994, 2004 and 2023. Remote sensing (RS), the Digital Shoreline Analysis System (DSAS), and Geographical Information System (GIS) were employed in the study, specifically focusing on the western coast of

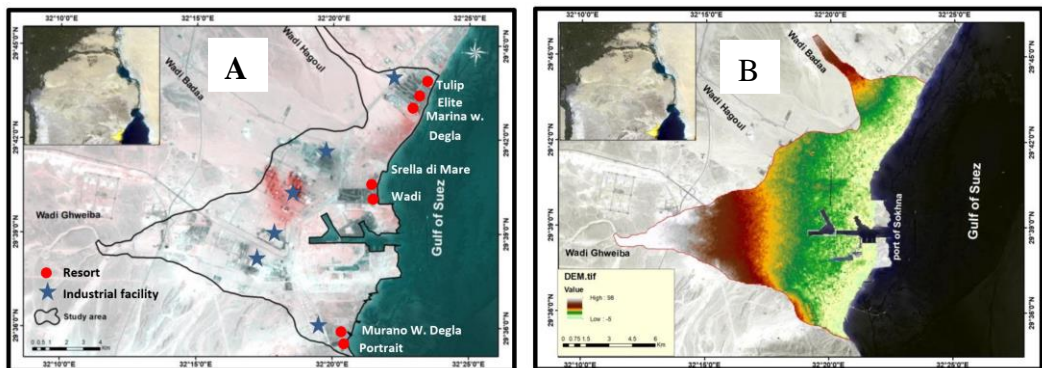
the Gulf of Suez in Egypt, from Ain Sokhna in the south to Wadi Bidaa in the north.

2- Aims

The current study aims to monitor human geomorphological changes over four decades during the period from 1984 to 2023, and the relationship of these changes to modern development processes in the Ain Sokhna area

3- Study Area

The study area is located in the eastern desert of Egypt on the western coast of the Gulf of Suez, about 50 km south of Suez, with a surface area of 171.2 km². The latitude and longitude of the study area are 29° 35' 55 " , 29° 41' 03 " N, and 32° 11' 16 " , 32° 22' 02 " E, respectively (Fig. 1).



Source :Landsat 9 OLI/TIRS , 2023.

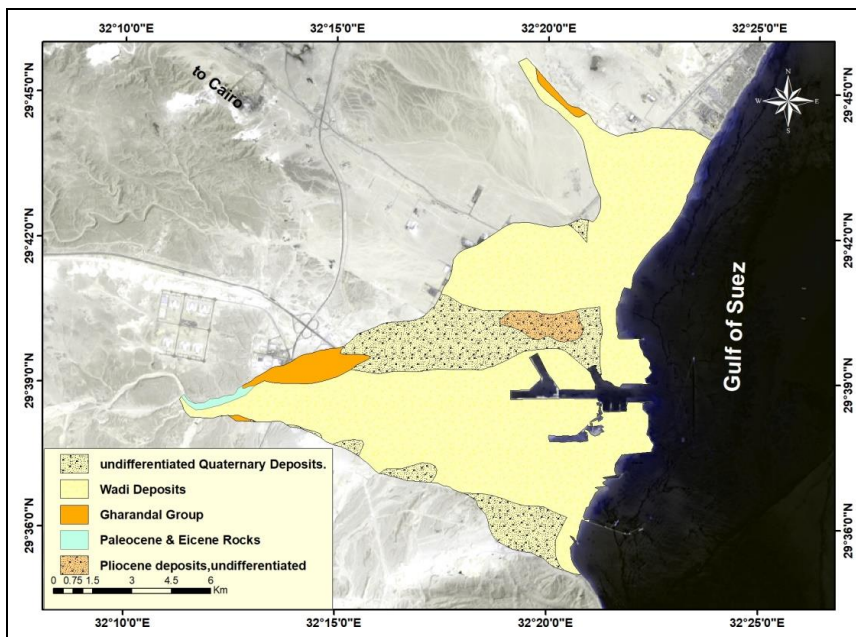
Source :SRTM DEM

(A) Study area

(B) Digital elevation model
of the study area

Figure 1.

Geologically, the coastal zone in this area is mainly composed of and covered by Quaternary deposits (Fig. 2). Structurally, the Gulf of Suez and northwestern Red Sea include several kilometer-scale tilted fault blocks bounded by NW-SE oriented major normal faults. The tilted fault blocks in the Suez Rift belong to three main provinces with different dip polarities, defining three mega-half grabens: two SW-dipping mega-half grabens in the northern and southern parts of the rift and an intervening NE-dipping mega-half graben (Moustafa & Khalil , 2020).



Source:., CONOCO (1987)

Figure 2. Geological map of the study area

4- Data and Methods

In this study, various geospatial data were utilized, such as optical satellite image and maps of different scales (topographic and geological maps). The study used remote sensing (RS), Digital Shoreline Analysis System (DSAS), and Geographical Information System (GIS).

4.1 Satellite Images

Basically, both the optical images of the Landsat mission and the optical images of the European Space Agency were utilized (Table 1). The optical images of the Landsat mission serve as a time archive dating back to 1972, while the European Space Agency's Sentinel-2 satellite provides recent optical images with a spatial resolution of up to 10 meters.

4.2 Maps

In the current research, a set of maps was used, which can be listed as follows:

- Geological Map, CONOCO Coral Company (1987), one sheet, scale 1/500,000.
- Geological Maps, The Geology of Egypt (2020), Various maps.

4.3 Remote Sensing Analysis:

The advancements in satellite remote sensing data have expanded its widespread applications across various fields. Remote sensing technology, using satellite imagery, offers a wide scope for monitoring different land use land cover (LULC) types to comprehend changes on Earth (Sekertekin et al., 2018). The remote sensing analyses in this study depended on the application of a set of spectral indices. The spectral index involves algebraic calculations of multispectral bands. It aims at automatic extraction of a specific feature (i.e. pixel-based features in the satellite image). Spectral indices allow one to extract land covers in the study area at different dates, such as built-up area, vegetation cover, and water bodies (Salem, 2018).

Table 1. Satellite images used in the current study

Satellite	Sensor	Date Acquired	Image (ID)	Band No.	spatial resolution (m)					
Landsat5	TM	1984/04/29	LT51760391984120FUI00	1-B	30					
				2-G						
				3-R						
				4-NIR						
				5-SWIR1						
				7- SWIR2						
				6- Thermal	120					
Landsat5	TM	1994/04/09	LT51760391994099FUI00	1-B	30					
				2-G						
				3-R						
				4-NIR						
				5-SWIR1						
				7- SWIR2						
				6- Thermal	120					
Landsat7	ETM	2000/04/10	LE71760392003100MTI00	1-B	30					
				2-G						
				3-R						
				4-NIR						
				5-SWIR1						
				7- SWIR2						
				6- Thermal	120					
				8-Panchromatic	15					
Landsat9	OLI_TIRS	2023/05/03	LC91760392023123LGN00	1-Coastal aerosol	30					
				2-B						
				3-G						
				4-R						
				5-NIR						
				6-SWIR1						
				7- SWIR2						
				9-Cirrus						
								8- Panchromatic	120	
								10- TIRS1	100	
								11- TIRS2		
Sentinel-2	MSI	2023/04/18	L2A_T36RVT_N0509_20230418T082609	2-B	10					
				3-G						
				4-R						
				8-NIR						
				5-VNIR						
				6- VNIR						
				7- VNIR						
				8a- VNIR						
				11-SWIR						
				12-SWIR						
				1- Ultra Blue	20					
				9- SWIR						
				10- SWIR						
				60						

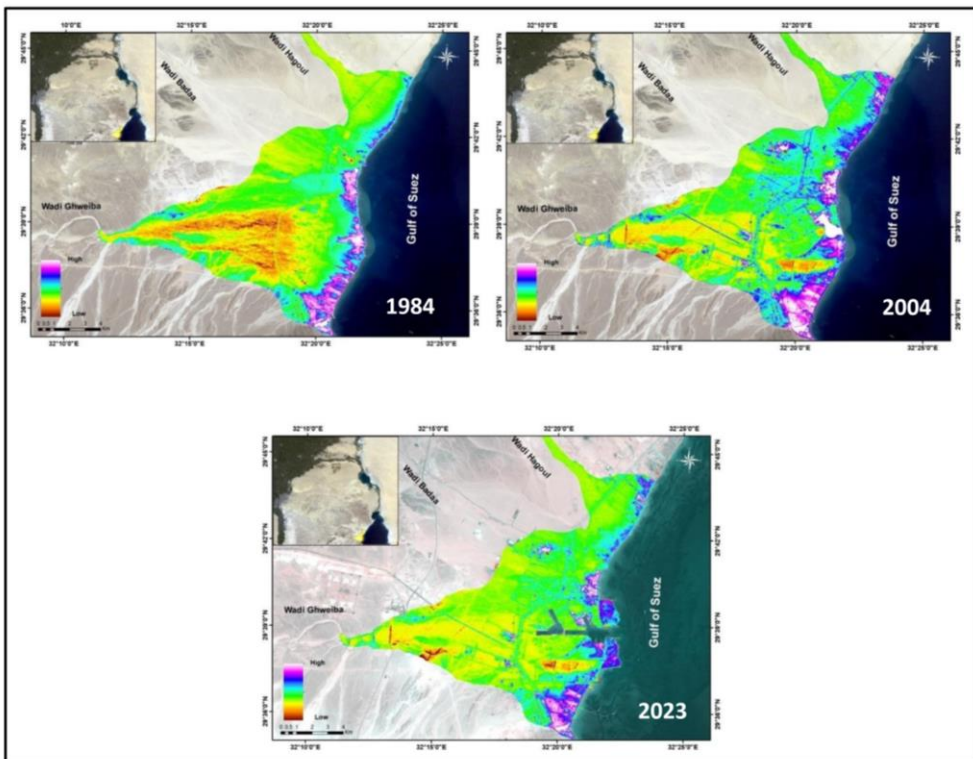
The current study utilizes the following spectral indices:

4.3.1 Enhanced Soil Salinity Index

El-Dessouky (2022) developed the Enhanced Soil Salinity Spectral Index (ESSI), which is based on the use of near-infrared (NIR) spectral reflection and short-wave infrared (SWIR)², it also involves subtracting the values of the Normalized Difference Vegetation Index (NDVI) (Fig. 3).

The ESSI is expressed as:

$$ESSI = \frac{NIR - SWIR2}{NIR + SWIR2} - NDVI$$



Source :Landsat images for 5 TM in 1984, 7 ETM in 2004 and 9 OLI/TIRS in 2023

Figure 3. Enhanced Soil Salinity Spectral Index (ESSI)

4.3.2 Built-Up Area Indices

To date, several techniques have been derived using satellite data to extract and calculate built-up areas and discriminate between built-up and non-built-up areas. Satellite remote sensing data with different temporal, spectral, and spatial resolution serve as invaluable resources for mapping built-up areas and monitoring urban growth and its impacts (Batty and Howes, 2001).

The use of built-up area indices is one of the practical applications of remote sensing data for distinguishing between built-up and non-built-up surfaces. Since the mid-1990s, numerous spectral built-up indices have been formulated for the rapid and accurate classification and monitoring of built-up lands using satellite data with different spatial and spectral resolutions (Estoque and Murayama, 2015) (Table 2).

The current study is based on the NDISI index (Fig. 4), which is based on differences in the spectral response between impermeable materials and other land features. Impermeable surfaces exhibit high daytime thermal response values and low near-infrared (NIR) and mid-infrared (MIR) reflectance values. Thus NDISI is expressed as

$$\text{NDISI} = \frac{T_{\text{lst}} - [(R_{\text{VIS}} + R_{\text{NIR}} + R_{\text{MIR}})/3]}{T_{\text{lst}} + [(R_{\text{VIS}} + R_{\text{NIR}} + R_{\text{MIR}})/3]}$$

Where

RNIR = NIR band

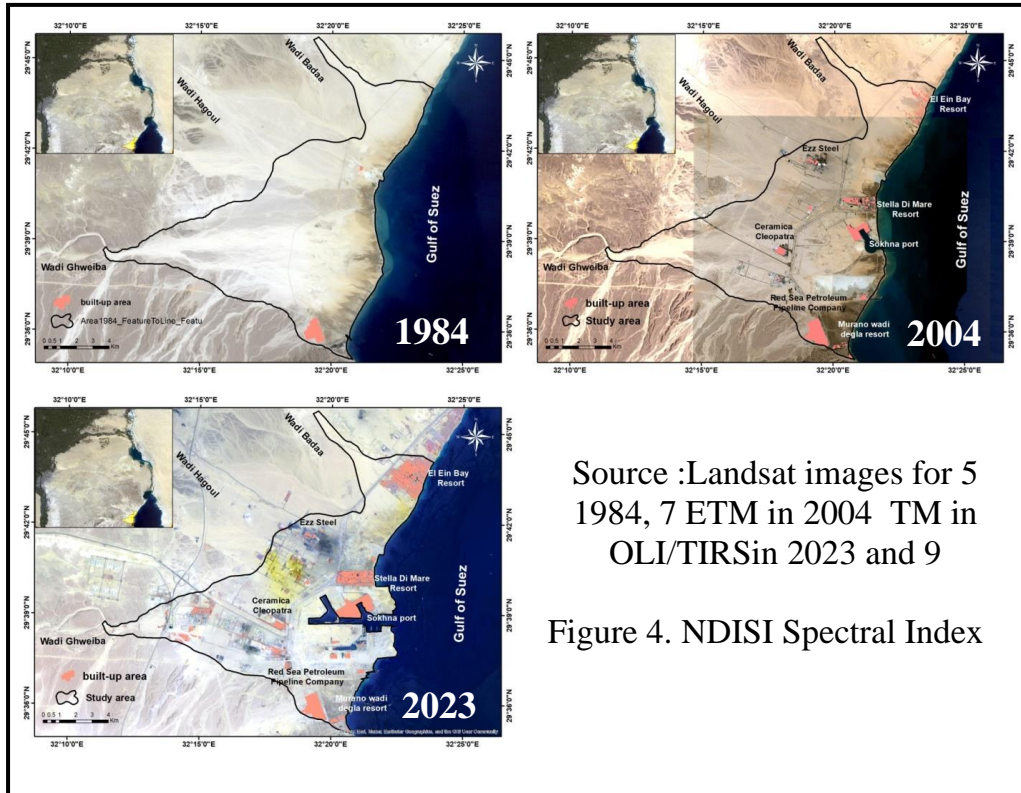
RMIR = MIR band

RVIS = one of the visible bands. Also, it can be expressed in MNDWI values

TLST = thermal surface temperature band

Table 2. built-up area indices formulas

Index	Formulae	Reference
UI	$\frac{(SWIR2 - NIR)}{(SWIR2 + NIR)}$	Kawamura, 1996
NDBI	$\frac{(SWIR1 - NIR)}{(SWIR1 + NIR)}$	Zha et al., 2003
NDBaI	$\frac{(SWIR1 - TIR)}{(SWIR1 + TIR)}$	Zhao and Chen, 2005
NBI	$\frac{(SWIR1 * RED)}{(NIR)}$	Chen et al., 2006
Improved NDBI	NDBIc - NDVIc c= continuous image	He et al., 2010
IBI	$\frac{(NDBI - (SAVI + MNDWI)/2)}{(NDBI + (SAVI + MNDWI)/2)}$	Xu, 2008
NDSI	$\frac{T_{1st} - [(R_{VIS} + R_{NIR} + R_{MIR})/3]}{T_{1st} + [(R_{VIS} + R_{NIR} + R_{MIR})/3]}$	Xu, 2010
EBBI	$\frac{(SWIR1 - NIR)}{10\sqrt{SWIR2 + TIR1}}$	As-Syakur et al., 2010
BRBA	$\frac{Red}{SWIR1}$	Waqar et al., 2012
NBAI	$\frac{(SWIR2 - \frac{SWIR1}{Green})}{(SWIR2 + \frac{SWIR1}{Green})}$	Waqar et al., 2012
VTPI	$\frac{NDWI}{(NDVI + NDBI)}$	Stathakis et al, 2012
VrNIR-BI	$\frac{(Green - NIR)}{(Green + NIR)}$	Estoque and Murayama, 2015
NgNIR-BI	$\frac{(Green - SWIR1)}{(Green + SWIR1)}$	Estoque and Murayama, 2015
MNDISI	$\frac{(TIRs - \frac{MNDWI + NIR + SWIR1}{3})}{(TIRs + \frac{MNDWI + NIR + SWIR1}{3})}$	Sun et al., 2017
BAEI	$\frac{(Red - 0.3)}{(Green + SWIR1)}$	Bouzekri et al., 2015
DBI	$\frac{(Blue - TIR1)}{(Blue + TIR1)} - NDVI$	Rasul et al., 2018



4.3.3 Surface Water Extraction Using Water Indices

In remote sensing techniques, there are numerous spectral indices used to extract water bodies or surface waters, such as the Normalized Difference Water Index (NDWI) (McFeeters, 1996), Modified NDWI (MNDWI) (Xu, 2006), Water Ratio Index (WRI) (Shen and Li, 2010), Normalized Difference Moisture Index (NDMI) (Gang and Dong-sheng, 2012), Automated Water Extraction Index (AWEI) (Feyisa et al., 2014), and New Water Index (NWI) (Ding et al., 2018)(table 3).

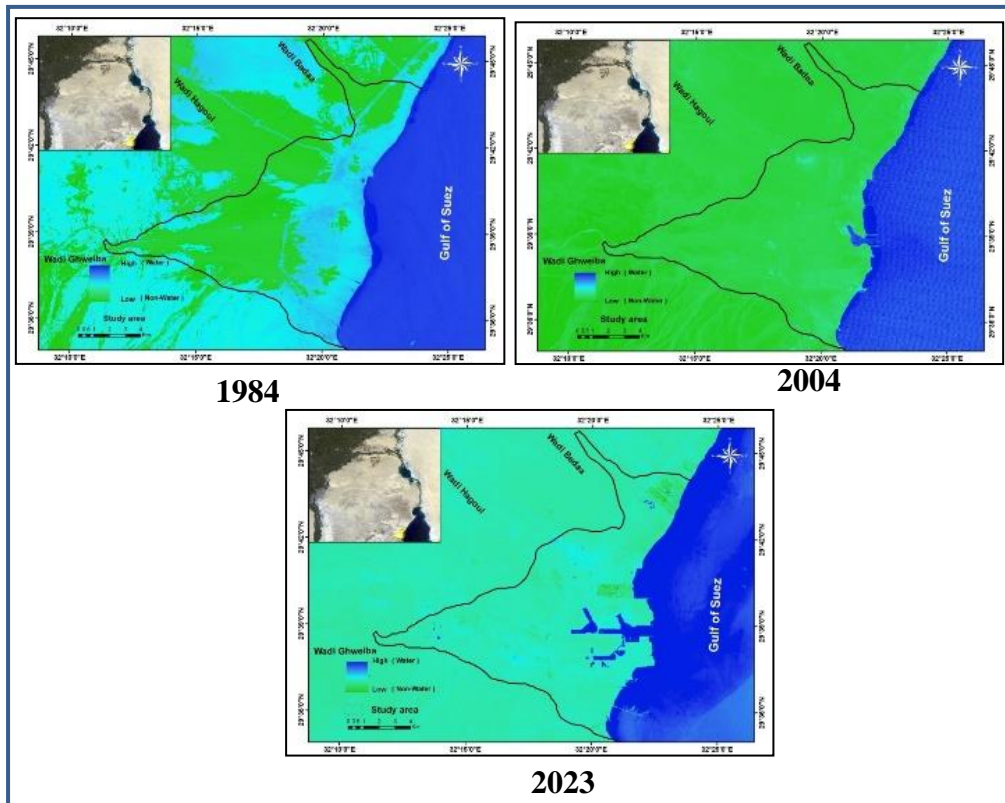
Table 3. Surface Water indices formulas

Index	Formulae	Reference
NDWI	$\frac{(Green - NIR)}{(Green + NIR)}$	McFeeters, 1996
MNDW	$\frac{(Green - SWIR1)}{(Green + SWIR1)}$	Xu, 2006
WRI	$\frac{(Green - Red)}{(NIR + SWIR)}$	Shen and Li, 2010
NDMI	$\frac{(NIR - SWIR)}{(NIR + SWIR)}$	Gang and Dong-sheng, 2012
AWEIsh	Blue + 2.5 × Green − 1.5 × (NIR + SWIR1) − 0.25 × SWIR2	Feyisa et al., 2014
AWEInsh	4 × (Green − SWIR1) − (0.25 × NIR + 2.75 × SWIR1)	

The NDMI index showed clear superiority in distinguishing water bodies from other land features, especially built-up areas and shadows (Fig. 5). Therefore, this study relied on it using the formula provided in the previous table.

4.3.4 Vegetation Cover Extraction Using Vegetation Indices

There are numerous vegetation cover Indices used in previous studies. However, the vegetation cover in the study area is characterized by gardens that have been planted as landscapes, either for resorts or industrial areas. These resorts extend along the Gulf coast where salt marshes (sabkhas) are present.



Source :Landsat images for 5 TM in 1984, 7 ETM in 2004 and 9 OLI/TIRS in 2023

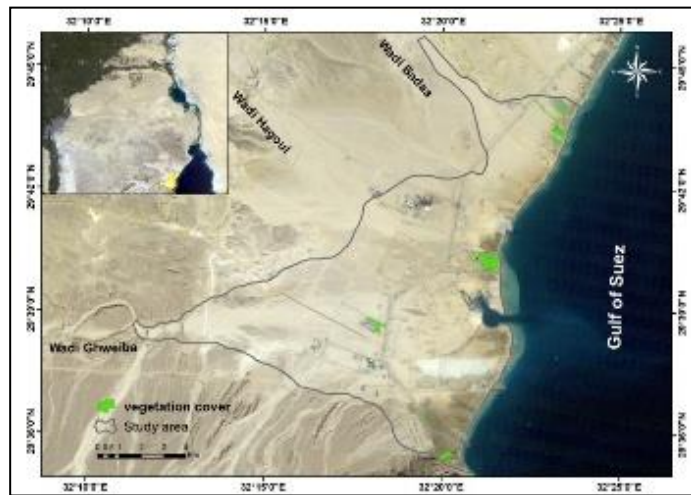
Figure 5. NDMI Spectral Index

Therefore, the Soil Adjusted Vegetation Index (SAVI) was used (Fig. 6), which is a corrected indicator for the Normalized Difference Vegetation Index. SAVI is utilized to account for the effect of soil brightness in areas with low vegetation cover. The SAVI is expressed as:

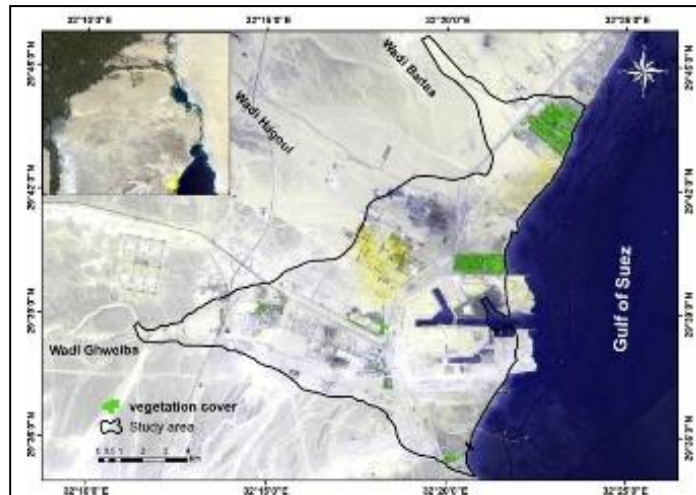
$$SAVI = ((NIR - R) / (NIR + R + L)) * (1 + L)$$

$$\text{In Landsat 4-7, SAVI} = ((\text{Band 4} - \text{Band 3}) / (\text{Band 4} + \text{Band 3} + 0.5)) * (1.5).$$

$$\text{In Landsat 8-9, SAVI} = ((\text{Band 5} - \text{Band 4}) / (\text{Band 5} + \text{Band 4} + 0.5)) * (1.5).$$



2004



2023

Source :Landsat images for 7 ETM in 2004 and 9 OLI/TIRS in 2023

Figure 6. SAVI Spectral Index

4.4 GIS Analysis :

A set of overlay analyses were employed, including symmetrical difference, update, union, intersection, and Identify, to perform spatial relationship analyses between extracted or digitized features and calculate the extent of morphological changes for these features.

5- Results and Discussion

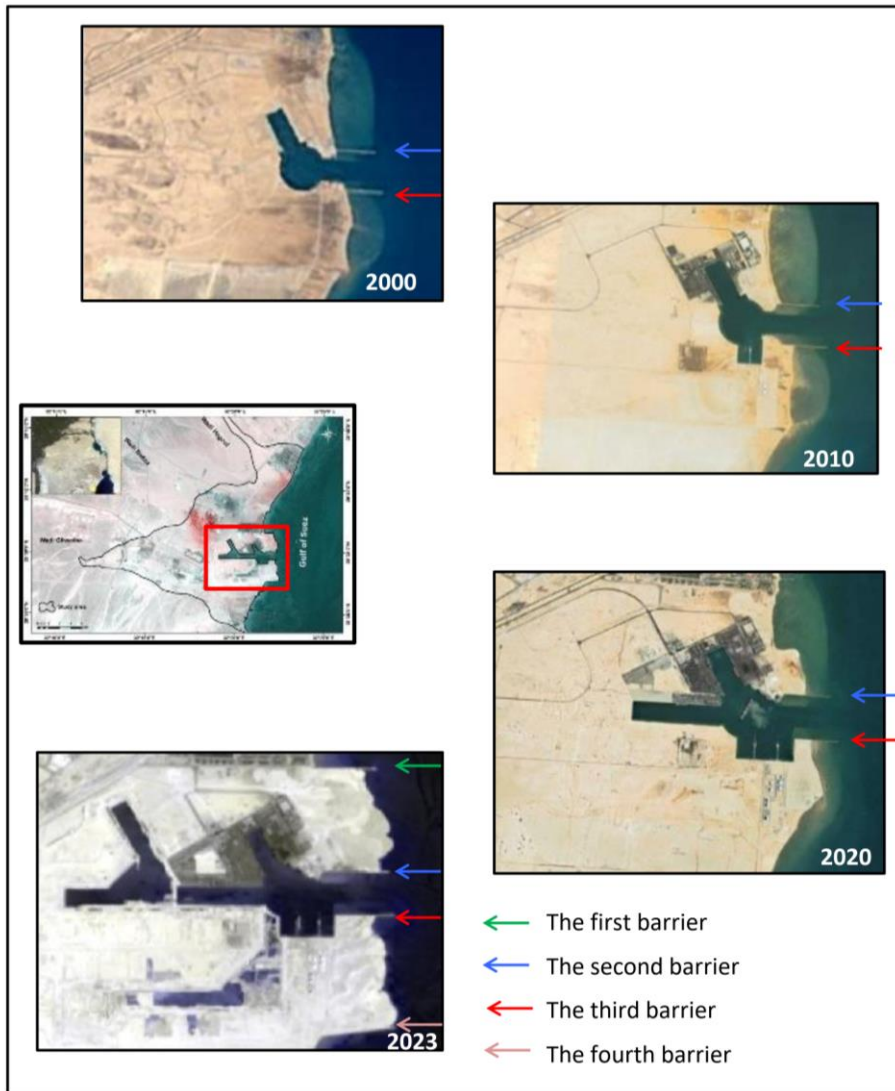
The study area is occupied by the Wadi Hagoul Fan, Wadi Badaa Fan, and the Delta of Wadi Ghweiba, all of which are natural geomorphological features formed by natural forces through the deposition of flood sediments, either along the Gulf coast or within it. The current study focuses on man-made geomorphological features that are associated with human exploitation of the region's resources, as follows:

5.1 Sokhna Port :

The port of Sokhna in the study area is considered one of the most important man-made landforms, as it involves man-made deposition, transportation, and man-made erosion.

- In 1984, the study area was completely barren. The actual work to establish the port of Sokhna began in 1991, and the drilling of the main basin of the port was completed in 2000.
- The total water surface area of the port basin increased from 0.86 km² in 2000 to 4.28 km² in 2023.
- Between 2000 and 2023, four breakwater barriers were constructed. One of them is located south of the port, and the second one is located north of the port. Additionally, there are two barriers, one to the north and one to the south of the port's navigational corridor (Fig. 7, 8).
- Between 2020 and 2023, the drilling outputs resulting from the expansion of the Sokhna port basins north and south of the first and second barriers began to be transported. The quantities of sand transported amounted to about 5 million m³ in 2023 with

the aim of acquiring new lands for the port, to be used later in establishing a logistical area within the national project to develop the Sokhna port.



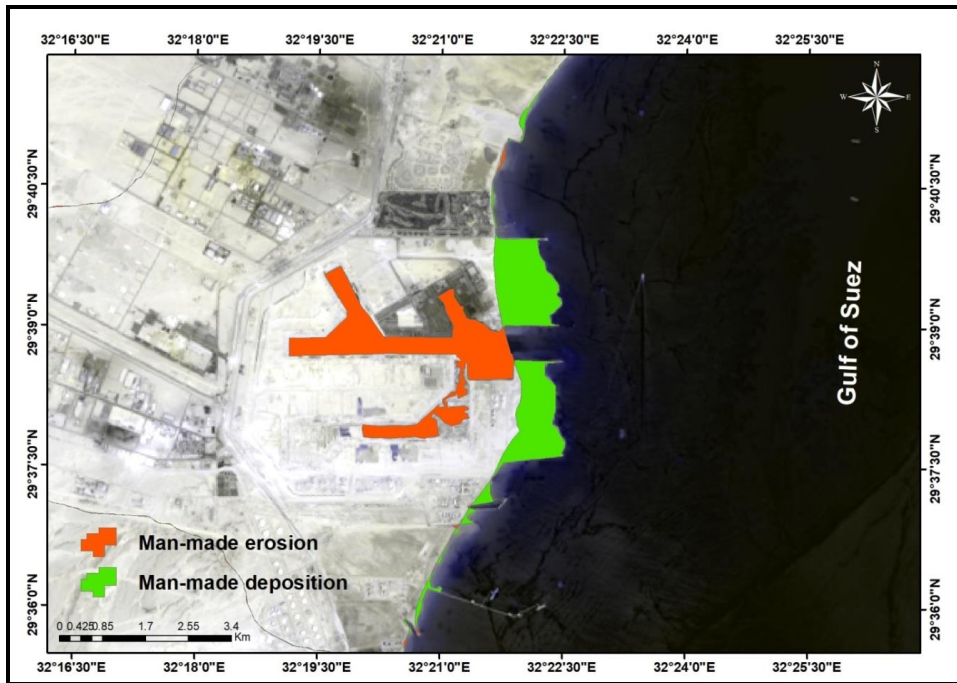
Source :Landsat images for 5 TM in 2000, 7 ETM in 2010, 8 OLI/TIRS in 2020 and 9 OLI/TIRS in 2023

Figure 7. Four breakwater barriers were constructed in Sokhna port between 2000 and 2023.



Figure 8. Barriers were constructed in Sokhna port between 2000 and 2023

- In general, the man-made landforms in the Sokhna port area between 1984 and 2023 can be classified into two main categories: man-made erosion, which amounted to 4,282 km², represented by the excavation of port basins, and man-made deposition, which amounted to 3,883 km², represented by the new lands that were added (Fig.9). Additionally, there has been a change in the urban area, with the administrative and service buildings in the port area increasing from 461 km² in 2000 to 1,443 km² in 2023.
- It is worth noting that the area of the sabkhas has fluctuated between increase and decrease. In 2004, the port of Sokhna and all its buildings occupied the coastal sabkha area. As more construction was done, the area of the sabkha decreased. This decrease continued until 2023, as the expansions, whether in buildings or the digging of new sidewalks, especially the southern ones encroached upon the area of the sabkha. However, the new land that has accumulated between the barriers is exposed to waterlogging by the Gulf waters and can be considered an area added to the sabkhas.



Source: Landsat images for 5 TM in 1984, and 9 OLI/TIRS in 2023.

Figure 9. Man-made erosion and deposition in Sokhna port between 1984 and 2023

In all honesty, it can be said that the man-made geomorphological changes that occurred on the shoreline in the port of Sokhna area during the years 1984 and 2023 surpass the total changes on the shoreline that resulted from natural processes along the eastern coast of the Red Sea and the Gulf of Suez in the same period.

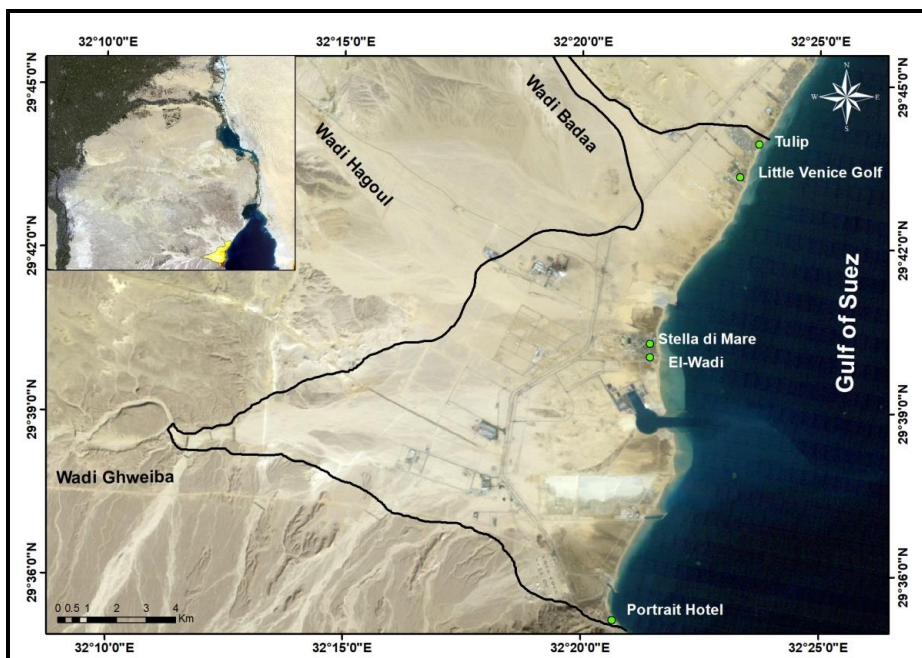
5.2 Urban Geomorphology:

The direct urban geomorphological process can be divided into erosion (damage) and accumulation (building). Specifically, the erosion process can be further categorized into excavation, flattening, and slope cutting operations. The accumulation process, on the other hand, can be categorized into construction, repair, and stacking (Jialin et al., 2017). Accordingly, the urban geomorphology features in the study area can be divided as follows:

5.2.1 Tourist Resorts

In 1984, the study area was completely devoid of any tourist resorts. However, in 2000, the construction of coastal resorts began in the study area and continued to increase until 2023, as indicated below:

- In 2000, the number of resorts in the study area reached five: from north to south, Tulip, Little Venice Golf, Stella Di Maria, The Valley, and Portrait Hotel. All of these resorts occupied the sabkha areas along the coast (Fig.10).

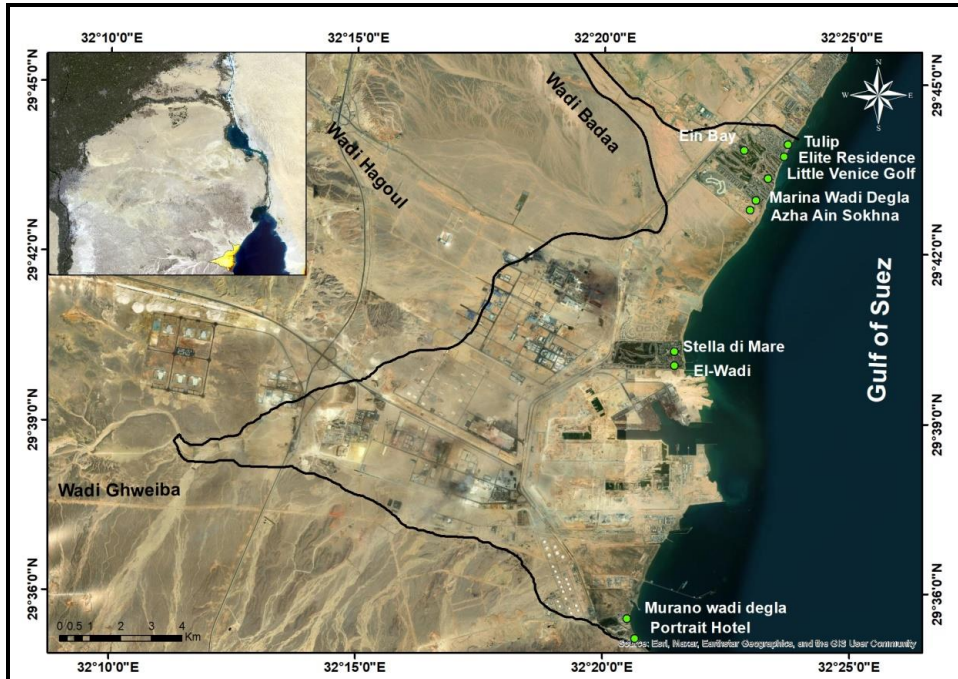


Sour :Landsat 7 ETM in 2004.

Figure 10. Tourist resorts in2000

- In 2023, the number of resorts doubled from five to ten from north to south, Tulip, Elite Residence, Ein Bay, Little Venice Golf, Marina Wadi Degla, Azha Ain Sokhna, Stella Di Maria, Wadi, Murano Wadi Degla, and Portrait Hotel. All of these resorts also occupied areas along the coast (marshes) (Fig.11).

- Between the two years, not only did the number of resorts double, but their area also expanded, whether it was the built-up areas or the vegetation (gardens). The built-up areas increased from 1993 km² in 2000 to 4123 km² in 2023, and the vegetation cover (gardens) increased from 2264 km² in 2000 to 4938 km² in 2023.



Source: Landsat 9 OLI/TIRS in 2023.

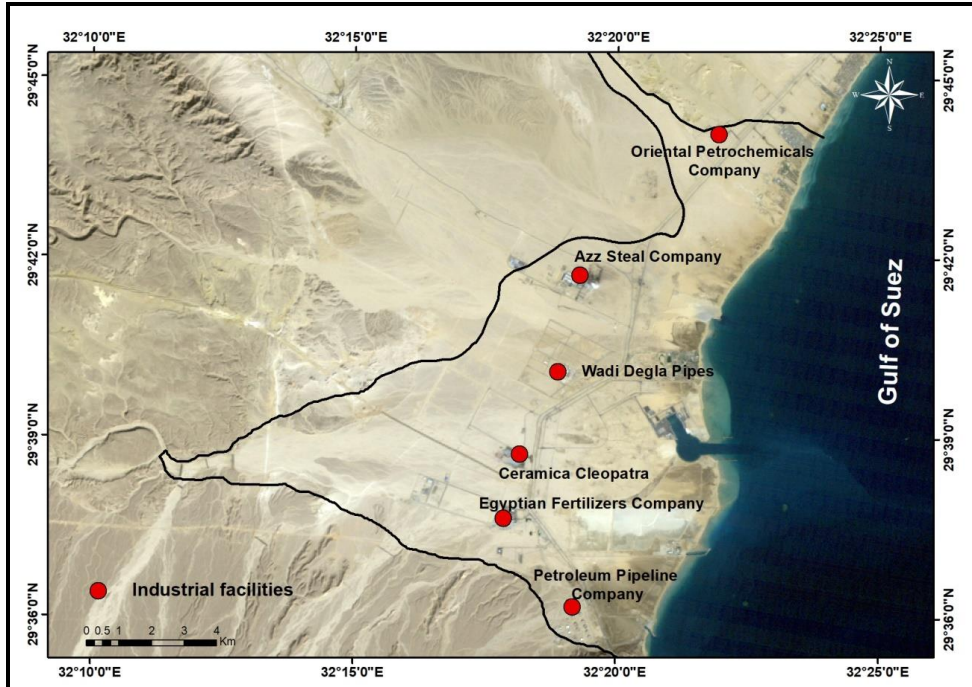
Figure 11. Tourist resorts in 2023.

5.2.2 Industrial facilities

The study area in 1984 only included the reservoirs of the Petroleum Pipeline Company - Red Sea in the south. Over time, by 2033, the study area became attractive to various industries.

- In 2004, there were only five industrial facilities, from north to south: Oriental Petrochemicals, Azz Steal, Wadi Degla Pipes, Ceramica Cleopatra, Egyptian Fertilizers, and Petroleum

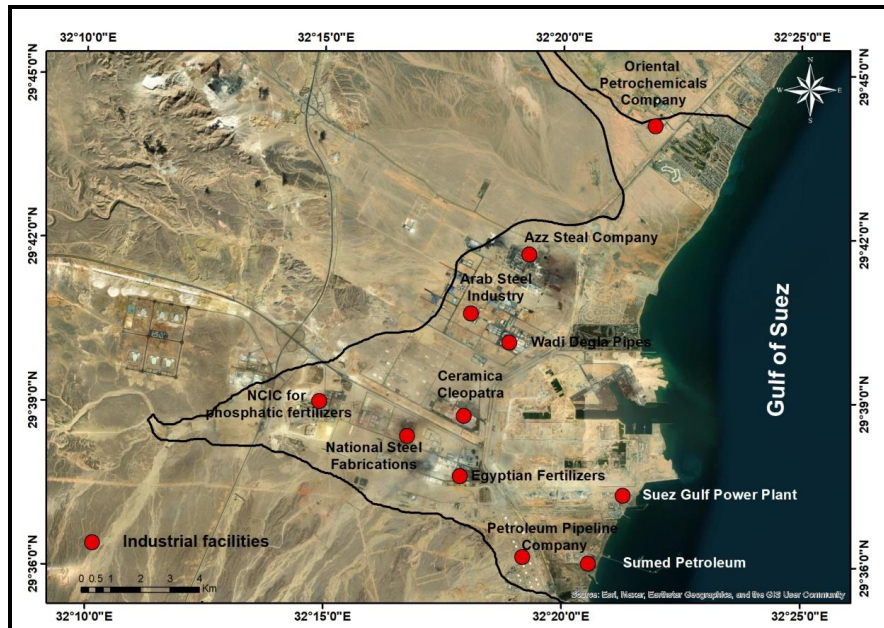
Pipeline. These facilities were distributed along a longitudinal axis with the Suez-Hurghada highway (Fig.12).



Sour :Landsat 7 ETM in 2004.

Figure 12. Industrial facilities in 2004

- In 2023, the number of industrial establishments significantly increased to about 40, distributed over the entire study area, especially after paving many roads linking the study area with other highways (Fig.13).



Source :Landsat 9 OLI/TIRS in 2023.

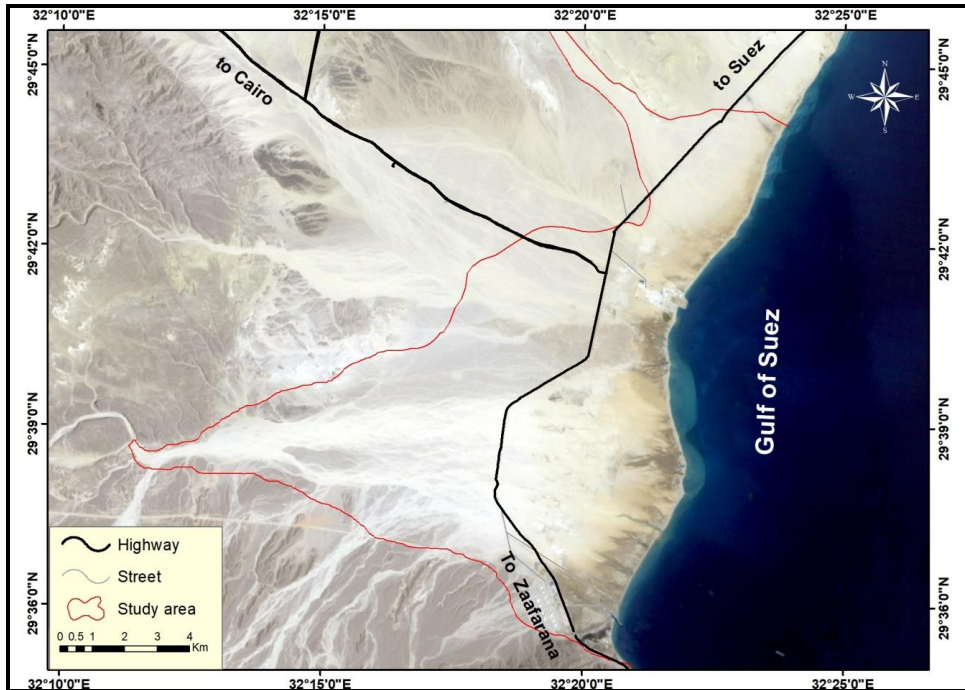
Figure 13. Industrial facilities in 2023

5.2.3 Transport Routes

The construction of a 1 km motorway section, 28 m wide, separated into 2 + 2 lanes (with 2 emergency lanes), requires 8 ha of land. During the construction, pits are dug, quarries are opened, and subsidiary roads built for the exploitation of building materials (Szabó and Lóczy, 2010). The construction of roads involves integrating erosion processes (cutting off the road paving rocks from their natural environment), the transportation of rocks and construction materials along the road to be built, and the accumulation of natural and unnatural materials. Finally, the roads are completed.

In 1984, only two roads crossed the study area: the Suez-Zafarana Road, with a length of 19.8 km and an average width of 11 m, consisting of one lane, and the Cairo-Ain Sokhna Road (Wadi Hajoul Road), with a length of 3.3 km and an average width of 9 m.

Additionally, there were three paved roads with a total length 5.4 km (Fig. 15) .



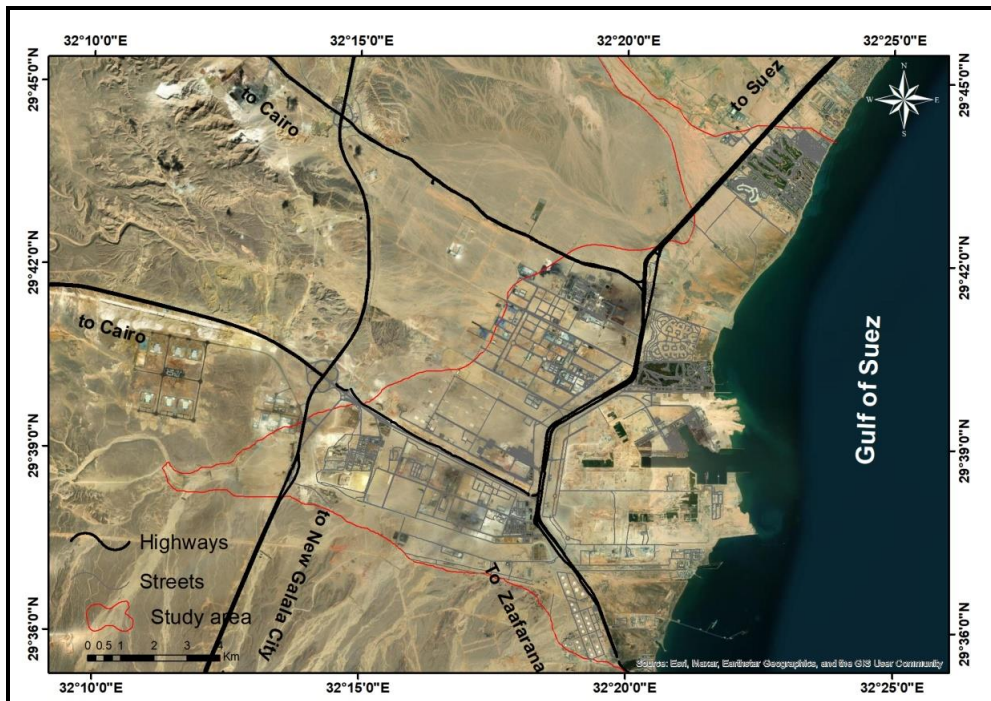
Source :Landsat 5 TM in 1984.

Figure 15. Transport Routes in 1984

With the construction of the Sokhna port, the number of paved roads and streets increased, and a new highway was built crossing the study area in 2004. This highway is the Cairo-Ain Sokhna (Katameya) road, with a length of 6.1 km and an average width of 33 m, consisting of two lanes. In 2023, Al-Jalala Highway constructed in the study area, with a length of 2.4 km and an average width of 35 m, consisting of two lanes (Fig. 16). Additionally, a significant number of streets were built, with a total length reaching 134.6 km (Fig. 17) .



Figure 15. Al-Jalala Highway in the study area.



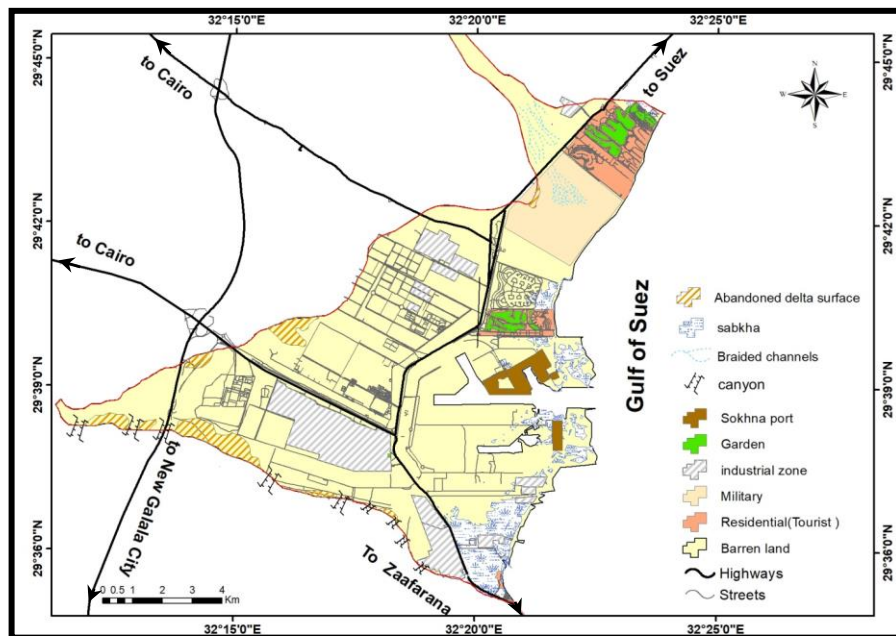
Source Landsat 9 OLI/TIRS in 2023.

Figure 15. Transport Routes in 2023

Conclusion

Outcomes of the current study indicate that the occurrence of anthropogenic geomorphological changes in the study area, whether it was the establishment of the Sokhna port, tourist resorts, industrial facilities, or transportation routes, was linked to the strategic importance of the study area. This importance began to increase in the early 2000s. These anthropogenic geomorphological features were interrelated.

As a result of the construction of the port, the study area became the focus of interest for various industries. Roads were paved to facilitate this development, and it subsequently became a highly suitable area for tourism investment. This transformation can be observed by comparing the barren state of the study area in 1984 with the anthro-geomorphological map of the study area in 2023 (Fig. 18).



Source :Landsat 9 OLI/TIRS in 2023.

Figure 18. Anthro-Geomorphological map of the study area in 2023

Anthropogenic activities in Egypt's Ain Sokhna area have significantly impacted the local coastal environment. These activities, including urbanization, industrial development, infrastructure construction, and tourism, have collectively contributed to geomorphological changes along the coastline. Ain Sokhna has experienced notable urban growth and the establishment of residential and commercial complexes, especially along the coastline. The construction of residential properties, hotels, and resorts has led to the transformation of natural shorelines and land reclamation from the sea. Tourism and recreational developments, including marinas, golf courses, and resorts, have expanded in the Ain Sokhna area (Table 4). These activities often entail land reclamation and the introduction of non-native vegetation, thereby altering the natural coastal ecosystem. Industrial zones and facilities, including ports, warehouses, and factories, have been established along the coast (Table 5). Moreover, the construction of ports and port facilities has involved dredging and changes in sediment dynamics, affecting coastal erosion and accretion patterns. The construction of coastal protection structures, such as seawalls, breakwaters, and groynes, has been employed to mitigate coastal erosion and protect infrastructure. While effective in the short term, these structures may alter natural coastal dynamics, posing long-term consequences for shoreline stability.

Table 4. Urban growth of Ain Sokhna between 2000 and 2023

	number of resorts	built-up areas (km ²)	vegetation cover (km ²)
2000	5	1993	2264
2023	10	4123	4938

Table 5. Area growth of Sokhna Port between 2000 and 2023

years	water surface (km ²)	urban area (km ²)
2000	0.86	461
2023	4.28	1,443

The development of road networks, utilities, and transportation systems has required land clearance and alterations (Table 6). The construction of roads and other infrastructure often results in habitat disturbance, changes in runoff patterns, and potential runoff change.

Table 6. Characteristics of transportation routes between 1984 and 2023 in the study area

	1984		2004	2023	
	Suez–Zafarana Road	Cairo–Ain Sokhna Road	Katameya road	Al–Jalala Highway	streets
length (km)	19.8	3.3	6.1	2.4	134.6
Average width (m)	11	9	33	35	

The construction of residential properties, hotels, and resorts has led to the transformation of natural shorelines and land reclamation from the sea. Industrial zones and facilities, including ports, warehouses, and factories, have been established along the coast. The development of road networks, utilities, and transportation systems has required land clearance and alterations. The construction of roads and other infrastructure often results in habitat disturbance, changes in runoff patterns, and potential runoff pollution. Moreover, the construction of ports and port facilities has involved dredging and changes in sediment dynamics, affecting coastal erosion and accretion patterns. The construction of coastal protection structures, such as seawalls, breakwaters, and groynes, has been employed to mitigate coastal erosion and protect infrastructure. While effective in the short term, these structures may alter natural coastal dynamics, posing long-term consequences for shoreline stability.

It is essential to note that while these anthropogenic activities have induced changes in the geomorphology of Ain Sokhna, they have also yielded economic benefits, employment opportunities, and infrastructural development. Striking a balance between development and environmental sustainability presents a challenge for policymakers, local communities, and stakeholders in the region.

Conducting comprehensive studies, monitoring activities, and adopting sustainable coastal management practices are crucial to minimizing the adverse impacts of anthropogenic activities on the coastal environment in Ain Sokhna, Egypt. These efforts aim to encourage responsible development, preserve natural ecosystems, and protect the long-term ecological health of the region.

References

- Batty M., & Howes D., (2001) Predicting temporal patterns in urban development from remote imagery. Taylor and Francis.
- El-Desouky, I., (2022) Determining the Effectiveness of Using Remote Sensing Indices to Deriving Sabkhas in Wadi An-Natrun Depression–Egypt. Faculty of Arts Journal. Port Said Univ., 19.19, 179-205.
- Estoque, R. C., & Murayama, Y. (2015). Classification and change detection of built-up lands from Landsat-7 ETM+ and Landsat-8 OLI/TIRS imageries: A comparative assessment of various spectral indices. *Ecological indicators*, 56, 205-217.
- Feyisa, G. L., Meilby, H., Fensholt, R., & Proud, S. R. (2014). Automated Water Extraction Index: A new technique for surface water mapping using Landsat imagery. *Remote sensing of environment*, 140, 23-35.
- Gang, W., & Dong-sheng, G. U. A. N. (2012). Effects of vegetation cover and normalized difference moisture index on thermal landscape pattern: A case study of Guangzhou, South China. *Yingyong Shengtai Xuebao*, 23(9).

- Hamimi, Z., El-Barkooky, A., Frías, J. M., Fritz, H., & Abd El-Rahman, Y. (Eds.). (2020). *The geology of Egypt*. Cham: Springer.
- Jialin, L., Lei, Y., Ruiliang, P., Yongchao, L. (2017). A review on anthropogenic geomorphology. *J. Geogr. Sci.* 27(1), 109-128.
- Khalil, S. M., & McClay, K. R. (2020). Extensional fault-related folding in the northwestern Red Sea, Egypt: segmented fault growth, fault linkages, corner folds and basin evolution. *Geological Society, London, Special Publications*, 476(1), 49-81.
- McFeeters, S. K. (1996). The use of the Normalized Difference Water Index (NDWI) in the delineation of open water features. *International journal of remote sensing*, 17(7), 1425-1432.
- Salem, A. (2018). The anthropogenic geomorphology of the new suburbs, East of Greater Cairo, Egypt. *Bulletin de la Société de Géographie d'Egypte*, 91(1), 1-28.
- Sekertekin, A., Abdikan, S., & Marangoz, A. M. (2018). The acquisition of impervious surface area from LANDSAT 8 satellite sensor data using urban indices: a comparative analysis. *Environmental monitoring and assessment*, 190, 1-13.
- Sekertekin, A., Abdikan, S., & Marangoz, A. M. (2018). The acquisition of impervious surface area from LANDSAT 8 satellite sensor data using urban indices: a comparative analysis. *Environmental monitoring and assessment*, 190, 1-13.
- Sekertekin, A., Cicekli, S. Y., & Arslan, N. (2018, October). Index-based identification of surface water resources using Sentinel-2 satellite imagery. In *2018 2nd international symposium on multidisciplinary studies and innovative technologies (ISMSIT)*, 1-5.

- Şekertekin, A., Marangoz, A. M., & Abdikan, S. (2018). Soil moisture mapping using Sentinel-1A synthetic aperture radar data. *International Journal of Environment and Geoinformatics*, 5(2), 178-188.
- Shen, L., & Li, C. (2010, June). Water body extraction from Landsat ETM+ imagery using adaboost algorithm. In 2010 18th International Conference on Geoinformatics, 1-4.
- Szabó, J., Dávid, L., & Lóczy, D. (2010). *Anthropogenic geomorphology: a guide to man-made landforms*. Springer Science & Business Media.
- Xu, H. (2006). Modification of normalised difference water index (NDWI) to enhance open water features in remotely sensed imagery. *International journal of remote sensing*, 27(14), 3025-3033.